Observation of Direct Dissociative Ionization in Molecular Hydrogen

B. L. G. Bakker,[1] D. H. Parker,[1] and W. J. van der Zande[2]

[1]*Department of Molecular and Laser Physics, University of Nijmegen, Toernooiveld, 6525 ED Nijmegen, The Netherlands*
[2]*FOM-Institute for Atomic and Molecular Physics, Kruislaan 407, 1098 SJ Amsterdam, The Netherlands*

(Received 24 July 2000)

Direct dissociative ionization is the simplest three-body breakup process in H_2. We describe the experimental verification of direct dissociative ionization to the repulsive $A^2\Sigma_u^+$ state by resolving the kinetic energy and angular distributions of the formed protons. A $(2 + 1)$ resonant enhanced multiphoton ionization process via the isotropic $E, F\,^1\Sigma_g^+(v = 6, J = 0)$ level is employed. The structure in the kinetic energy spectrum is well described by a projection of the vibrational wave function of the $E, F\,^1\Sigma_g^+(v = 6, J = 0)$ state onto the repulsive ionic state. The electronic character of the ionization continuum is revealed by the proton angular distribution.

DOI: 10.1103/PhysRevLett.86.3272 PACS numbers: 33.80.Gj, 33.80.Rv, 34.50.Gb

In excitation of molecular hydrogen above the $H + H^+$ dissociation limit molecular ions may be formed, or also two neutral H atom fragments, or three particles, an electron, proton, and H atom, can be produced. This last process may involve two steps, where the first step is the formation of a neutral doubly excited state from which molecular dissociation commences. The second step is then the autoionization of this dissociating state, forming an $H\text{-}H^+$ pair. Alternatively, dissociative ionization may be a direct process, in which H_2 is excited to the ionic dissociation continuum of H_2^+ (the $A\,^2\Sigma_u^+$ state). Dissociative photoionization, both *direct* and *indirect*, leads to three free particles (H, H^+, e^-). Hence, these processes are asymptotically nondistinguishable. Moreover, as the energy may be distributed over the three particles, neither the electron nor the heavy particle kinetic energy spectrum will reveal sharp distinctive structures. While dissociative ionization occurs in all molecules, hydrogen is the simplest three-body system. A search for this process requires an analysis of both kinetic energy and angular distributions of the photofragments.

Photoexcitation of H_2 has been the subject of extensive experimental research using XUV ($\lambda < 150$ nm) one-photon excitation [1–5]. The introduction of intense strong laser systems made it possible to populate different intermediate high lying states via multiphoton excitation pathways, from which dissociation and ionization can be driven with less energetic photons. Experiments have been reported via the $B\,^1\Sigma_u^+$ state (using one or three photons) [6,7] and via the $E, F\,^1\Sigma_g^+$ state (using two photons) [8–10]. In many of these studies, doubly excited neutral states [11,12] positioned in the ionization continuum have key roles, masking the observation of direct dissociative ionization.

In this letter we present kinetic energy distributions (KED) as well as the angular distributions (AD) of the protons formed in one-photon dissociative photoionization from the $E, F\,^1\Sigma_g^+(v = 6, J = 0)$ state, which is produced with two other photons from the molecular ground state. The oscillatory structure in the proton KED is explained as a projection of the bound vibrational wave function on the repulsive $A\,^2\Sigma_u^+$ ionic state. The technique of velocity map imaging combines the simultaneous recording of KED and AD of the formed protons. Velocity map imaging has been used extensively in photodissociation studies, where fragments are ionized using multiphoton processes [13]. In this study, $(2 + 1)$ resonant enhanced multiphoton dissociative ionization forms ions directly. In the following, we provide some details on the excitation step and the experimental setup followed by a description and discussion of the experimental results.

Direct dissociative ionization is the excitation of the repulsive, $A\,^2\Sigma_u^+$, ionic state (arrow in Fig. 1). Here the ejection of the electron and molecular dissociation occurs simultaneously. This process is more likely when starting from the outer well of the E, F state using photons of 193 nm. At this same energy, repulsive neutral states may

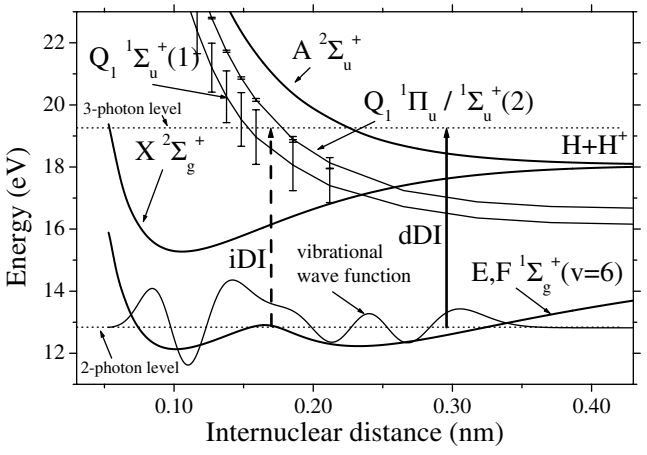

FIG. 1. Schematic potential energy diagram. The E, F potential is from Ref. [19]. The doubly excited states are presented including their autoionization linewidths as error bars, taken from Tennyson [12]. Also shown is the vibrational wave function of the intermediate state at the two-photon level. The vertical arrows represent *indirect* dissociative ionization (iDI, dotted line) and *direct* dissociative ionization (dDI, solid line) at the three-photon level.

 0031-9007/01/86(15)/3272(4)$15.00

be excited. Here, dissociation partially precedes ionization (dashed arrow in Fig. 1). In this case, autoionization involves the dissociation continuum of the H_2^+ electronic ground state. Photoexcitation from the E, F state (see Fig. 1) may also result in the formation of bound H_2^+ ions from the inner well region. The use of the rotationless $J = 0$ level provides a complete isotropic intermediate population, facilitating the description of the AD of the resulting protons. The AD intensity $I(\theta) \propto 1 + \beta[\frac{3}{2}\cos^2\theta - \frac{1}{2}]$ depends on the angle θ between the laser polarization direction and the velocity vector of the fragments and can be characterized [14] by one anisotropy parameter, β, which ranges between the limiting values -1 to 2. This parameter determines the symmetry of the transitions.

The velocity map imaging apparatus used has already been described in detail elsewhere and a summary of the experimental details will be given here. A pulsed supersonic beam of pure H_2 is directed down the axis of a time-of-flight (TOF) mass spectrometer, and crossed at right angles by the counterpropagating laser light of a line-narrowed ($\delta\nu \approx 0.5\ \mathrm{cm}^{-1}$) [15] tunable ArF excimer laser set on the $E, F\,^1\Sigma_g^+(v = 6, J = 0) \leftarrow\leftarrow X\,^1\Sigma_g^+(v = 0, J = 0)$ two-photon transition in hydrogen. A subsequent photon can then excite the hydrogen above the $H^+ + H$ dissociation limit at a total photon energy of 19.26 eV, forming protons. The 193 nm light (15 ns pulse width, 25 mJ per pulse) was focused onto the molecular beam, resulting in an intensity of $\approx 5 \times 10^{10}\ \mathrm{W/cm^2}$. The laser light was more than 99% vertically polarized. The formed protons were extracted from the ionization region into the grounded time-of-flight tube and detected on a two-dimensional microchannel plate/phosphor screen detector read by a CCD camera. Mass selectivity was achieved by increasing the gain of the detector when the H^+ ions arrive. The image (sum of 25 000 shots) is inverted (from the two dimensions of the detector to all three spatial dimensions) by using an inverse Abel transformation. This is possible because of the presence of a symmetry axis (the polarization direction of the light, vertical to the TOF axis, parallel to the detector surface). We note that even in the narrow band mode the laser intensity still consists of 50% narrow band light on top of a broad band background. Hence, the third (one-)photon step will be "polluted" with a broad band component. The resolution (ΔKE/KE) of the apparatus can be as high as 2% [13]. The excimer laser used has an unfavorable rectangular beam shape, resulting in a decreased resolution with a value of $\Delta E/E \approx 8\%$ [15].

As mentioned above, after three-photon absorption at 19.26 eV, the hydrogen molecule can decay in three major pathways: dissociation into two neutrals (D), ionization forming an H_2^+ ion (I), and *direct* or *indirect* dissociative ionization (DI). For dissociative ionization the maximum kinetic energy release over the fragments is determined by the ionic dissociation limit at 18.07 eV and is therefore 1.19 eV. In dissociative ionization the electron also carries away kinetic energy. Hence, the H^+ ions are expected in the energy range from 0 to 0.6 eV ($= 1.19/2$ eV). In the case of molecular dissociation (D), a ground state H atom is formed together with an excited fragment. These excited atoms are partially ionized by the strong 6.42 eV laser light. Their kinetic energy is determined by the dissociation limit of $H(n = 1) + H(n > 1)$ and will have discrete values between 0.6 eV [$H(n = \infty)$] and 2.29 eV [$H(n = 2)$]. Molecular ionization (I) produces initially, $H_2^+\ X\,^2\Sigma_g^+(v^+) + e^-$. The energy of the photon allows H_2^+ to be formed in all v^+ levels. A fraction of these molecular ions can be photodissociated, again yielding a proton. The kinetic energy of the protons is determined by the initial vibrational level, and ranges from 1.88 to 3.2 eV. Hence, in an energy resolved KED spectrum all pathways are distinguishable.

A measured image is presented in Fig. 2. The intensity of the signal from low to high corresponds to from black to white as denoted in the gray scale in Fig. 2. The direction of the laser polarization is along the y axis. The image clearly shows rings with relatively large diameter (high KE values) and three fainter rings with small diameters (low KE values). The angular distribution can be observed directly. The outer rings show an intensity peaking along the laser polarization in accordance with a $\cos^2\theta$ angular distribution ($\beta = 2$) as expected for the $A\,^2\Sigma_u^+ \leftarrow X\,^2\Sigma_g^+$ ionic dissociation process. The inner rings are more isotropic. In Fig. 3 these data are transformed into a KED (plotting the intensity as a function of the radius of the ring). Figure 3(a) reveals the full range and all three processes. Figure 3(b) concentrates on the energy region for DI. Structures are seen both in the DI region and the I region.

The structure in the ionization region (I) matches photodissociation of the hydrogen ion formed in a distribution

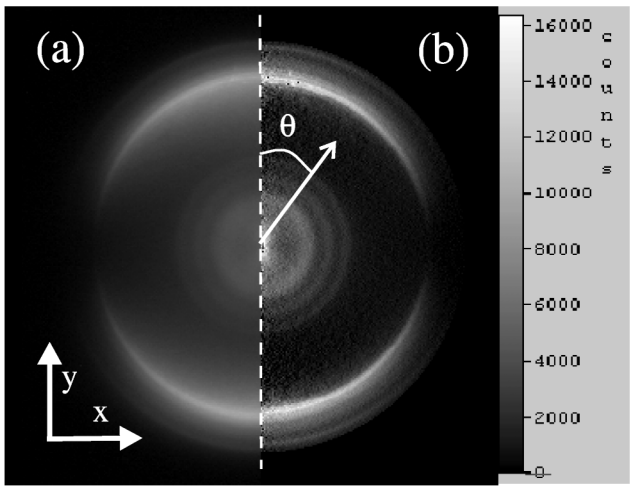

FIG. 2. (a) Measured image. (b) Abel transformed image. The angle θ is between the dotted line (presenting the laser polarization) and the fragments. On the right side an intensity gray scale is presented.

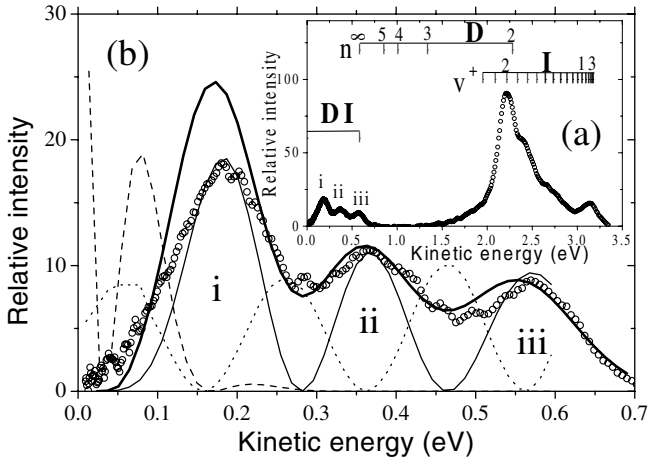

FIG. 3. Kinetic energy distributions. (a) The inset shows the full energy region, revealing DI and I. (b) The main figure shows the region below 0.7 eV. A small background due to the inverse Abel transformation has been subtracted. The three peaks in the DI region are denoted with *i*, *ii*, and *iii*. The measured KED is presented by open circles. The lines are calculated KED distributions using different models. The thin solid line, direct DI via the A state; dashed line, direct DI via the *X* state, dotted line, approximate indirect DI via $Q_1\,^1\Pi_u$; thick solid line, direct DI via the *A* state with experimental broadening.

peaked at the $H_2^+\ X\,^2\Sigma_g^+(v^+ = 2)$ and $H_2^+\ X\,^2\Sigma_g^+(v^+ = 13)$ states. Their production is enhanced in accordance with the v^+ dependent Frank-Condon (FC) factors with the $E,F(v = 6)$ level. This has been seen in photoelectron spectra (the complement of our KED) by Xu *et al.* [9]. No evidence is found for the formation of H($n \geq 3$) fragments from the dissociation (*D*) process. The H($n = 2$) could be hidden below the *I* peak. Also Xu *et al.* [9] found no evidence for formation of excited H atoms due to dissociation [9]. Important for the discussion later, the absence of *D* fragments suggests that the doubly excited states do not play a dominant role at this wavelength. The signal in the DI region below 0.7 eV in Fig. 3 shows oscillatory structure, which cannot be assigned to known states or known dissociation limits. In the following we argue that this structure is the consequence of a *direct* DI process. Xu *et al.* [9] did not report oscillations in their photoelectron spectrum, not being sensitive in the associated photoelectron energy region. The possible DI processes can be summarized as follows. From the $E,F(v = 6)$ state, the following states are one-photon allowed: the doubly excited $Q_1\,^1\Sigma_u^+$ and $^1\Pi_u$ states and the ionic dissociative continua of the $X\,^2\Sigma_g^+$ and $A\,^2\Sigma_u^+$ states. At the internuclear separations in the outer "*F*" well, the electron configuration of the E,F state is dominated by the $(2p\sigma_u)^2$ configuration. As a consequence, at these internuclear separations, excitation to the ionic $A\,^2\Sigma_u^+[(2p\sigma_u)]$, and to the doubly excited $^1\Sigma_u^+[(2p\sigma_u)(2s\sigma_g)$, and $(2p\sigma_u)(3d\sigma_g)]$ and $^1\Pi_u[(2p\sigma_u)(2d\pi_g)]$ are all one-electron transitions.

The process of *direct* DI leads to a KED of the proton given by $I(E_P) = P_{\rm el}(E_{\rm tot} - 2E_P) \times |\langle\chi_{EF^2\Sigma_g^+}(R) \mid \chi_{A^2\Sigma_u^+}(R;2E_p)\rangle|^2$, with $P_{\rm el}$ ($E_{\rm el}$) describing the probability of generating a photoelectron with energy $E_{\rm el}$; $E_{\rm tot}$ is the energy available for the three particles. This function was approximated by the H(1*S*) photoionization curve which is finite at threshold, and then slowly decreases with electron energy [16]. The factor 2 (in $2E_P$) comes from the fact that the kinetic energy is equally divided over the H and H^+ fragments. As mentioned, the photons couple the outer (*F*) well with the dissociative ionization continuum in a one-electron transition [$2p\sigma_u \rightarrow \varepsilon$ (s or d)λ_g]. We assume the excitation probability to be independent of internuclear separation. Figure 3(b) shows the results. The position and shape of the $v = 6$ vibrational level is found by numerically solving the Schrödinger equation using a Numerov method. The same procedure was used to determine the FC factors.

The loss of structure is due to the finite resolution of the apparatus. The magnitude of the instrumental resolution can be appreciated from the signal above 0.6 eV (the maximum allowed kinetic energy for the proton). This experimental broadening is used to adjust the calculated KED (thin solid line) in Fig. 3(b) resulting in the broadened calculated KED (thick solid line). This KED reproduces the measured KED very well. Only the height of peak i differs which could be due to an *R* dependence of the transition dipole moment. In principle, a small part of the signal may also be due to alternative ionization pathways, such as *direct* DI into the continuum of the ionic ground state [4,5], or *indirect* DI via the doubly excited states. The former process has much smaller FC factors in combination with a very different energy dependent behavior [see dashed line in Fig. 3(b)].

Indirect DI via the $[(2p\sigma_u)(2s\sigma_g)$ and $(2p\sigma_u)(3d\sigma_g)]$ $^1\Sigma_u^+$ states and the $[(2p\sigma_u)(3d\pi_g)]\,^1\Pi_u\ Q_1$ states is possible [11,12]. Tennyson [12] reported autoionization (aI) widths of all these states. In the case of a large aI width, and hence very fast autoionization, autoionization precedes dissociation and the observed KED of the protons will be indistinguishable from direct DI into the ionic ground state. This is the case for the first $^1\Sigma_u^+$ state. In the case of a small aI width, most of the molecules will dissociate prior to ionization (process *D* in Fig. 1). A small fraction will autoionize during dissociation. The KED is given by the FC factors between the dissociative continuum states in the $Q_1\,^1\Pi_u \backslash\, ^1\Sigma_u^+$ at the three-photon level and the $H_2^+\ X\,^2\Sigma_g^+$ state at variable energy ($2E_p$) [17]: $I(E_p) \simeq |\langle\chi_{Q_1}(R;3h\nu) \mid \chi_{XH_2^+}(R;2E_p)\rangle|^2$. Figure 3(b) shows the results for all three doubly excited states, revealing a clear mismatch with experiment. Exact calculations of the competition between aI and dissociation of the neural doubly excited states is beyond the scope of this experimental work. Such calculations have been performed for the case dissociation from the $B\,^1\Sigma_u^+$ state [18].

Direct dissociative ionization to the continuum of the electronically excited ionic state reproduces our results well, as seen in Fig. 3(b). The oscillations then reflect the behavior of the wave function of the outer well (*F* side) of

the $E, F\,^1\Sigma_g^+(v = 6, J = 0)$ state. It is possible that indirect processes also contribute to our observed signal. In the following we further corroborate this interpretation with the expected angular behavior. The angular distributions of the three dissociative ionization peaks *i*, *ii*, and *iii* result in the following anisotropy parameters: $\beta(i) = 0.1 \pm 0.1$, $\beta(ii) = 0.0 \pm 0.1$, and $\beta(iii) = -0.1 \pm 0.1$. These values are about 0, *a priori* surprising in the case of one-photon bound-free transitions, where limiting values are expected. Theoretically the angular distribution is easily estimated. The initial state in the one-photon dissociation process is completely isotropic ($J = 0$). This facilitates calculation of the AD considerably. Ionization of the $2p\sigma_u$ electron can generate an electron with *s*-wave and *d*-wave character. In the case of an *s*-wave electron, the nuclei must carry the angular momentum of the photon. Elementary angular momentum algebra gives a value for the anisotropy parameter, β, being $\beta = 2$, maximally aligned. In the case of a *d*-wave electron, the electron carries most of the angular momentum of the photon, reducing the anisotropy parameter of the nuclei considerably. Angular momentum algebra indeed gives a strongly reduced anisotropy parameter of $\beta = 0.2$. Finally it is, in principle, possible that the electron and molecular ion exchange angular momentum in such a way that the $H - H^+$ pair is left with three units of angular momentum ($N^+ = 3$) after emission of the electron. This channel is expected to give an AD given by $\beta = 0.8$.

The observed angular distributions are very close to $\beta = 0.2$. We conclude that in *direct* DI the ion is left in a dissociative state with $N^+ = 1$ and that a *d*-wave electron is emitted. In the united atom limit, the ionization process concerns a *p* electron; in the united atom picture the *p*-*d* transition is 30 times stronger than the *p*-*s* transition. The small discrepancy between the $\beta = 0.2$ and the observed slightly negative values may be attributed to instrumental effects connected to the background subtraction. Excitation of the autoionizing $^1\Pi_u$ doubly excited state would reduce the anisotropy parameter, as this adds perpendicular ($\beta = -1$) character. This effect is diminished by the simultaneous parallel excitation to the $^1\Sigma_u^+$ state. The associated KED does not fit, however, and it has been argued before that this channel is unlikely because of the absence of detectable neutral H($n = 3$) fragments.

In conclusion, we have shown that oscillatory structure directly reflects the outer well vibrational wave function of the E, F state in *direct* dissociative ionization of H_2. The identification of this process is further corroborated by the angular distributions of the observed protons. Hence, two continua are simultaneously excited, with a resulting structure in the KED and also in the associated photoelectron spectra characteristic of direct dissociative ionization.

This work was part of the research program of the "Stichting voor Fundamenteel Onderzoek der Materie (FOM)" and is financially supported by the "Nederlandse Organisatie voor Wetenschappelijk Onderzoek (NWO)." The authors thank M. C. van Beek, N. J. Dam, and J. J. ter Meulen for help and the use of the tunable excimer laser, C. Sikkens and C. Timmer for technical support, and Dr. F. Robicheaux for clarifying discussions.

[1] S. Strathdee and R. Browning, J. Phys. B **12**, 1789 (1979).
[2] K. Ito, R. I. Hall, and M. Ukai, J. Chem. Phys. **104**, 8449 (1996).
[3] Z. X. He, J. N. Cutler, S. H. Southworth, L. R. Hughey, and J. A. R. Samson, J. Chem. Phys. **103**, 3912 (1995).
[4] J. H. D. Eland, M. Takahashi, and V. Hikosaka, Faraday Discuss. **115**, 119 (2000).
[5] K. Ito, J. Adachi, R. Hall, S. Motoki, E. Shigamasa, K. Soejima, and A. Yagishita, J. Phys. B **33**, 527 (2000).
[6] J. W. J. Verschuur and H. B. van Linden-van den Heuvell, Chem. Phys. **129**, 1 (1989).
[7] H. Rottke, J. Ludwig, and W. Sandner, J. Phys. B **30**, 4049 (1997).
[8] S. Yang and W. T. Hill III, Phys. Rev. A **51**, 2301 (1995).
[9] E. Xu, A. P. Hickman, R. Kachru, T. Tsuboi, and H. Helm, Phys. Rev. A **40**, 7031 (1989).
[10] W. T. Hill III, B. P. Turner, S. Yang, J. Zhu, and D. L Hatten, Phys. Rev. A **43**, 3668 (1991).
[11] S. L. Guberman, J. Chem. Phys. **78**, 1404 (1983).
[12] J. Tennyson, At. Data Nucl. Data Tables **64**, 253 (1999).
[13] A. T. J. B. Eppink and D. H. Parker, Rev. Sci. Instrum. **68**, 3477 (1998).
[14] R. N. Zare, Mol. Photochem. **4**, 1 (1972).
[15] B. L. G. Bakker and D. H. Parker, J. Chem. Phys. **112**, 4037 (2000).
[16] T. F. Gallagher, *Rydberg Atoms* (Cambridge University Press, Cambridge, UK, 1994), p. 41.
[17] This FC factor does not converge but oscillates. The mean value of this oscillation is used.
[18] K. R. Dastidar and R. K. Das, J. Chem. Phys. **112**, 3689 (2000).
[19] L. Wolniewicz and K. Dressler, J. Chem. Phys. **100**, 444 (1994).